Measurement of GPS Derived Precipitable Water Vapour (PWV) in Low and High Altitudes in Nepal.

[1]Kuber Saud*†, [1]Nabin Sah†,[1]Basu Dev Ghimire; [1]Balaram Khadka; Shreeram Nagarkoti; [2]Aakash Pokheral; [3]Narayan P. Chapagain

[1]Department of Physics, St. Xavier's College, Maitighar, Tribhuvan University

[2]Central Department of Physics, Tribhuvan University

[3]Amrit Campus, Tribhuvan University

*Corresponding author(s): 021bscphy007@sxc.edu.np

(Received: September 12, 2024; Revised: December 12, 2024)

† Both authors contributed equally

Abstract

The study of precipitable water vapour (PWV) using satellite data and ground-based observation is crucial for understanding hydrological processes, atmospheric circulation, and weather systems. It is considered the most prominent greenhouse gas in the Earth's atmosphere. It is highly variable in both space and time across the Earth. Precipitable Water Vapor is a measure of the total amount of water vapour present in a vertical column of the atmosphere from the Earth's surface to the top of it. This study investigates the potential atmospheric water vapour column at high (JMSM)and low(GRHI) to understand water vapour dynamics. To investigate precipitable water vapour, GNSS/GPS data were downloaded from UNAVCO SAGE. The downloaded data were processed and analyzed using GAMIT/GLOBK software which is a comprehensive GPS analysis package developed at the Massachusetts Institute of Technology (MIT), the Harvard-Smithsonian Center for Astrophysics (CfA), and the Scripps Institution of Oceanography (SIO). The main purpose of this software is to process data for Atmospheric science. This paper's findings investigate the PWV amount in high and low altitudes over a year. Our finding shows that there is a significant difference in PWV levels between the two stations, with low-altitude areas exhibiting higher humidity and precipitation during the monsoon season, while high-altitudes show reduced water vapour concentrations influenced by surrounding climatic variation.

Keywords: *Precipitated water vapour(PWV), Global Positioning System (GPS), Zenith Hydrostatic Delay (ZHD) Remote sensing*

1. Introduction

Nepal's vast topography, which extends from the plain lowland terrain to the towering mountains, offers distinct challenges and opportunities for meteorological studies (Chapman, 2024). One critical aspect of atmospheric science is the measurement of precipitated water vapour, which plays a vital role in weather patterns, climate change, and hydrology (Pokharel, 2023; Ghimire et al., 2024). This article explores the use of Global

Positioning System (GPS) data to measure precipitated water vapour in both low and high-altitude regions of Nepal.

The atmosphere is a combination of gases that surrounds the Earth. It makes life possible by providing us with air to breathe, protecting us from harmful ultraviolet (UV) radiation coming from the Sun. Furthermore, the atmosphere plays a pivotal role in trapping heat and maintaining a livable temperature environment (Ghimire et al., 2022). Without it, the Earth's temperature would be similar to that of the moon, which experiences extreme temperature fluctuations between day and night (-208°F to 250°F) due to the lack of an atmosphere (Priester et al., 1960). As we know, water vapour in the atmosphere varies frequently as well as highly in both domain time and space.

Precipitable water vapour is the amount of condensed water in a column of humid air over a unit cross-sectional area (Manabe & Wetherald, 1967). Water vapour in the atmosphere is of central importance in several ways: for instance, it plays the leading role in the balance of planetary radiation; it affects and responds to atmospheric motions, while it also plays a significant role in many aspects of atmospheric processes acting over enormous spatial and temporal scales (Neelin et al., 2022). Atmospheric water vapor has a significant impact on atmospheric water transport, energy transformation, and other climatic phenomena, therefore it is purposeful to track and comprehend its changing circumstances and mechanism. PW affects aerosols' optical characteristics, causing water cycles, energy transfer, clouds, and rain (Raval & Ramanathan, 1989, Chen et al., 2022). By playing a crucial role in cloud formation, PWV in the atmosphere not only affects the water balance but also significantly affects the heat balance in the atmosphere by modifying radiation through mechanisms such as absorption, scattering, and reflection (Obregón et al., 2021; Ghimire et al., 2022).

The GPS signal bends away from the norm when it enters the troposphere due to a change in medium density, which covers a greater area than the shortest geometric path. ZTD is the total delay in the zenith direction of the GPS signals. ZHD and ZWD are the two parts that make up the ZTD. While ZWD is brought on by atmospheric water vapour, ZHD is the delay in the signal caused by dry gases such as oxygen, nitrogen, etc. While ZWD can be assessed by processing the GPS data using various processing techniques such as Precise Point Processing (Zumberge et al., 1997), ZHD can be computed depending on the atmospheric characteristics using empirical models and observation of Double Difference (Rocken et al., 1993). Finally, we can assess PWV in the specified time and space once we get the ZWD.

The motivation behind doing this research is to fill the gap of utilising GPS for the water vapour measurement in a country like Nepal where almost a significant portion of people rely on agriculture, which is directly affected by the precipitated water vapour. Accurate measurement of PWV can improve weather forecasting.

2. Materials And Methodology

Nepal has a vast geographical structure as well as vast climatic variation. The measurement of PWV in Nepal is significantly important in terms of knowing the atmospheric water vapour pattern. Our research focuses on Nepal's high and low altitudes, including the grhi(low) and jmsm (high). These stations have been selected due to their distinct climatic and geographical characteristics, which allow researchers to analyze atmospheric conditions across different altitudes and regions.

2.1. Data

GPS consists of 28 satellites distributed in different six orbital planes transmitting L-band radio signals of wavelength ranging from 19 cm to 22 cm. IGS (International GPS Service) network includes more than 100 global stations which provide orbit determination of 5cm accuracy. Radio waves when passing from the atmosphere get reflected and if 'μ' is the reflective index of light then the phase refractivity can be found (Kursinski et al., 2020)

$$N = 77.6\ P/T + 3.73\ 105\ Pw\ /T\ 2 - 4.03\ n_e\ /f\ 2 \qquad \text{.....(1)}$$

Where N is the refractivity which is $(n-1)x10^6$ and T is the temperature. P is total pressure and P_W is partial pressure of water vapor in hectopascal. Here, the variable the free electron density in electrons per cubic meter and the signal frequency in Hertz.

In this study we have used ground-based observation in this method dual dual-frequency signal is received at a ground-based receiver and is used to analyze the signal delay which determines the water vapour in the path from the GPS satellite and receiver (Bevis et al., 1992; Businger et al., 1996; Rocken et al., 1993)

For this study, we have taken ground-based receivers at high altitudes and low altitudes.

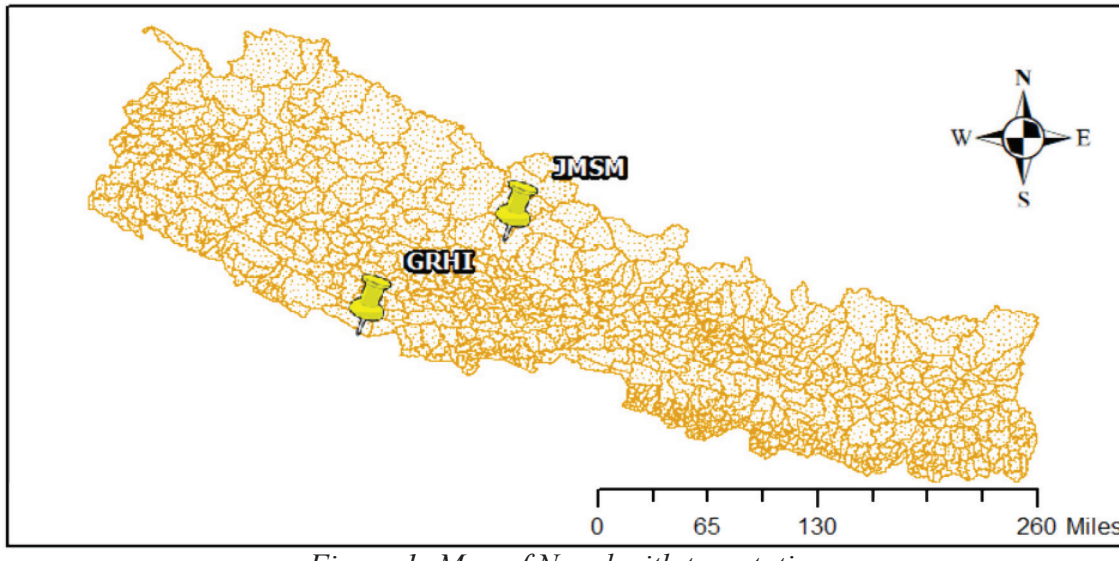

Figure 1: Map of Nepal with two station

Table 1: GPS station details:

Station Name	Latitude	Longitude	Altitude
GRHI	27°57'03.6"N	82°29'27.6"E	729.3932 m
JMSM	28°48'18.0"N	83°44'34.8"E	3438.266 m

For this study, we have downloaded data from UNAVCO in RINEX format for 365 days and processed using GAMIT software. We then use different scripts to obtain the required data (Herring et al., 2002).

2.2 Method

Precipitate Water Vapor can be derived from GPS by the total delay of the GPS signal known as Zenith Total Delay which can be measured by the ground-based receiver (Bevis et al., 1992, 1994; Hagemann et al., 2003). GPS stations and GPS satellites are rarely in Zenith but the delay can still be measured using a mapping function (Niell, 1996). Where the mapping function is inversely proportional to the sine of the elevation angle; and ZTD is the sum of ZHD and ZWD.

$$ZTD = ZHD + ZWD \quad \text{……..(2)}$$

where ZHD is Zenith Hydrostatic Delay

ZWD is Zenith Wet Delay

Zenith Wet Delay can range from a few millimetres to 350mm ranging from extremely dry conditions to extremely humid conditions and its primary cause is due to the permanent dipole moment of water vapour whereas the Zenith Hydrostatic Delay has a magnitude of roughly 2300mm and is linked to the atmosphere's induced dipole moment. The ZHD can be computed as a function of the surface pressure p_S at GPS antenna height, assuming hydrostatic equilibrium (i.e., the gravity force is balanced by the pressure gradient)

$$ZHD = (2.2768 \pm 0.0005)\, p_s / f(f,H) \text{.....(3)}$$

Where The dependency of gravity acceleration on surface height above the ellipsoid 'H' and latitude 'ϕ' is taken into account by f.

We can relate the PWV and ZWD and can be given by a conversion factor $\prod$:

$$PWV = ZWD\ \Pi = (ZTD–ZHD)\Pi \text{.....(4)}$$

Also,

$$\Pi^{-1} = 10^{-6}\, \rho_{H2O}\, R_v\, (C_1 + T_m C_2)/T_m \text{ .....(5)}$$

Where ρ_{H2O} is liquid water density

R_v is a specific gas constant of water vapour C_1 & C_2 are constant
T_m is the weighted atmospheric mean temperature

from (Bevis et al., 1994) C_1 =(3.739±0.012) 10^5 $^0K^2$ hPa^{-1} and C_2 =(22.1±2.2) $^0K^2$ hPa^{-1}

And T_m can be calculated using the vertical profile of pressure, and temperature of water vapour and has a linear relationship with station temperature observation T_s.

$$T_m \approx 70.2 + 0.7T_s \quad \text{.....(6)}$$

3. Result and Discussion

The two GPS stations (i) GHRI and (ii) JMSM situated in the western part of Nepal at low and high altitudes have shown significant differences in precipitated water vapour amount.

Time-series result of GRHI

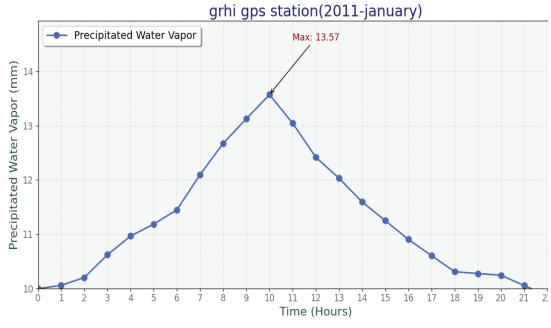

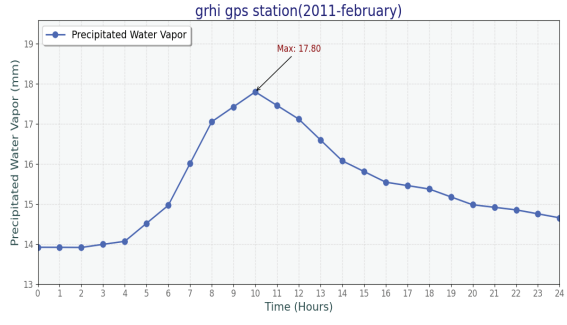

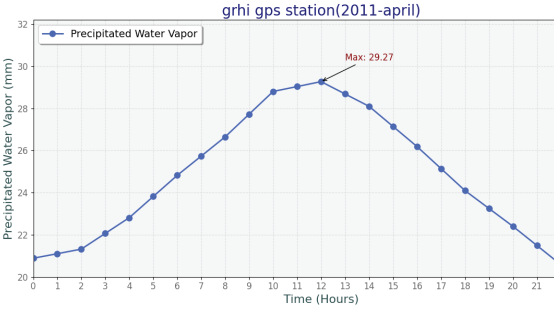

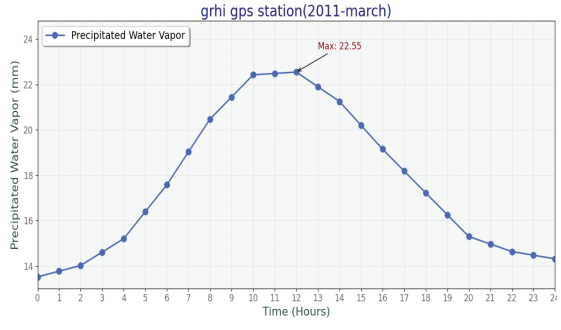

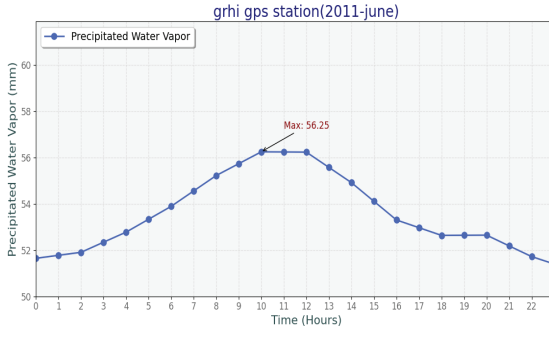

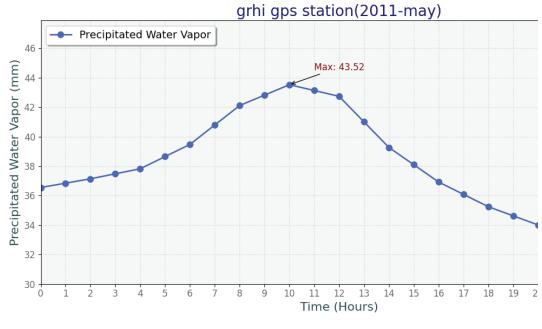

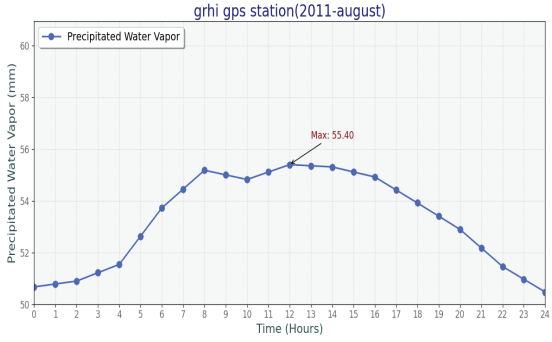

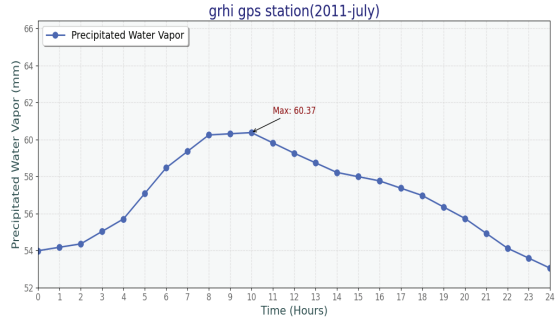

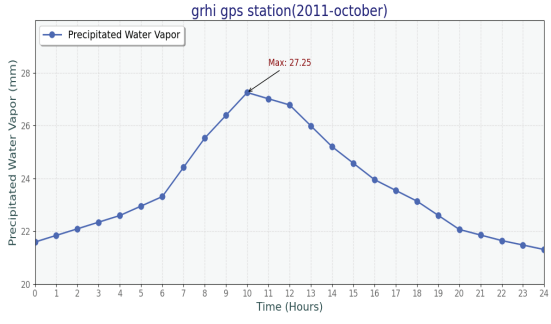

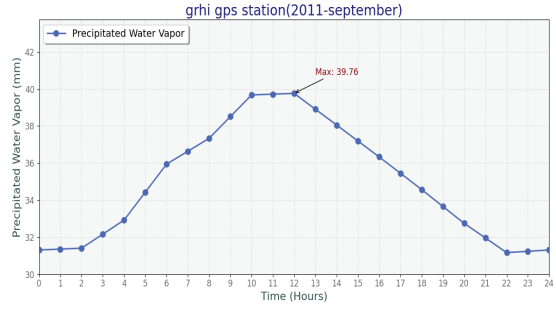

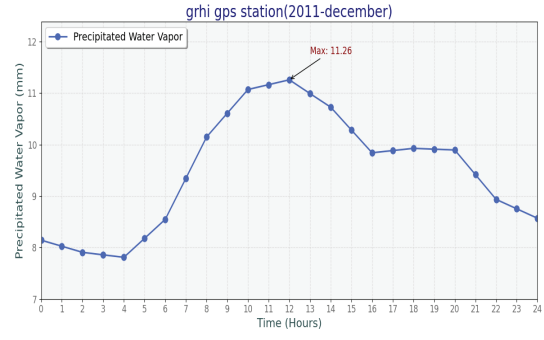

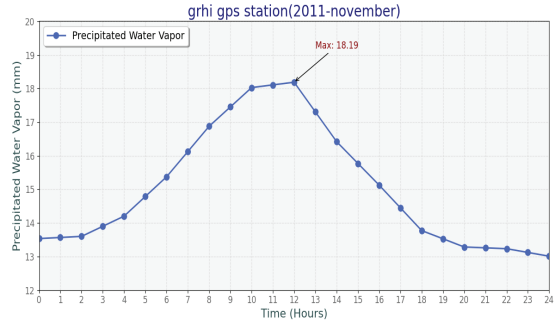

From the above graph, we can observe that the maximum precipitated water vapour is seen in July ie 60.37 mm during the period of 8-10 am whereas the minimum PWV is obtained in December. Further, it is noted that in every month of 2011, the precipitated water vapour starts increasing from the dusk of the morning and reaches a maximum in the period of 8-12 PM and then slowly decreases. We can also observe a similar pattern in the months that is the precipitated water vapour increases from January and reaches a maximum in July and then slowly decreases till December.

Time series graph of JMSM

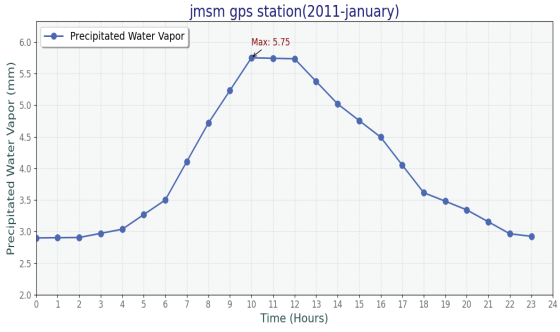

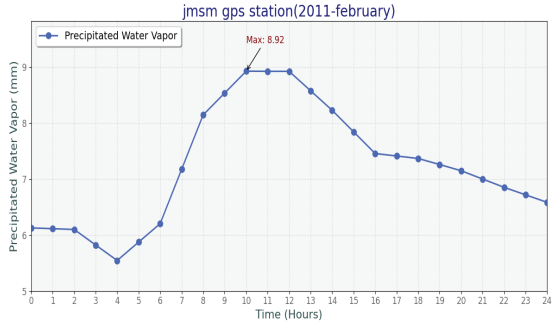

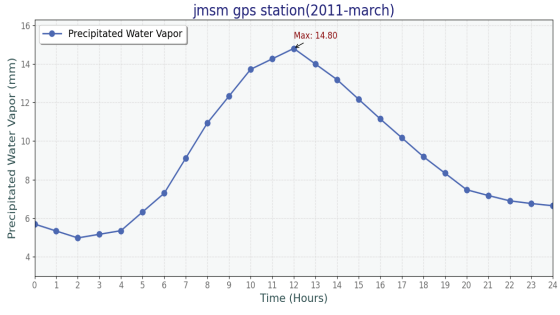

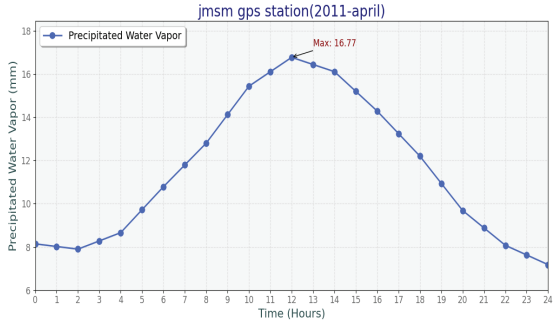

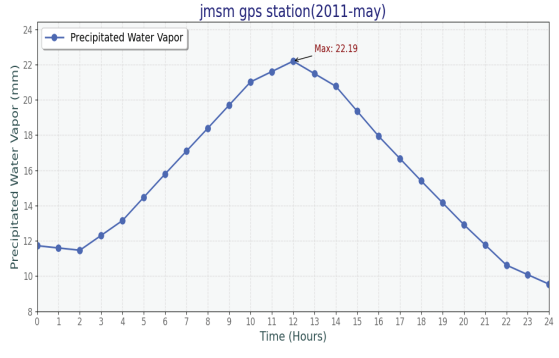

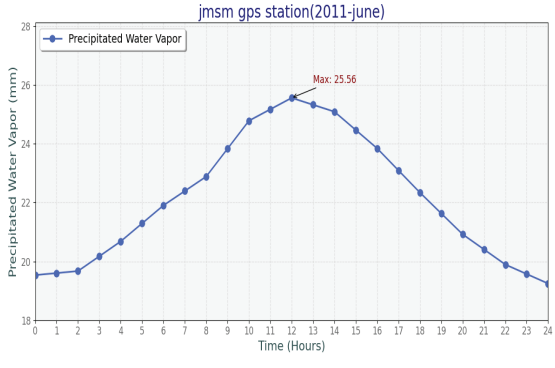

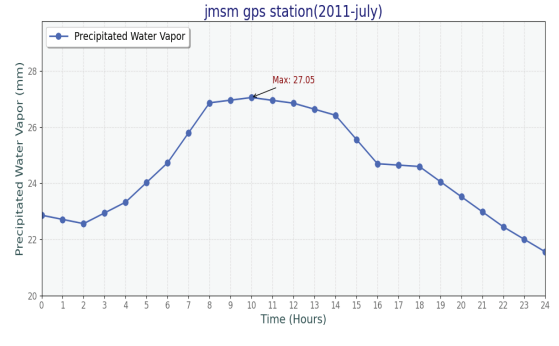

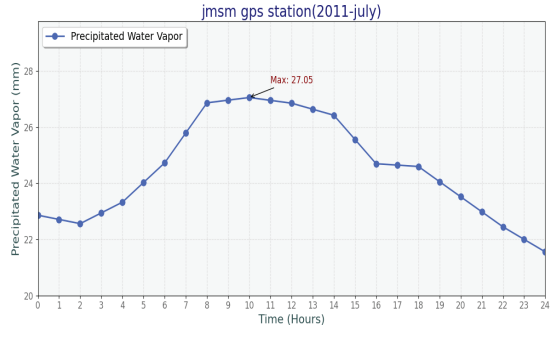

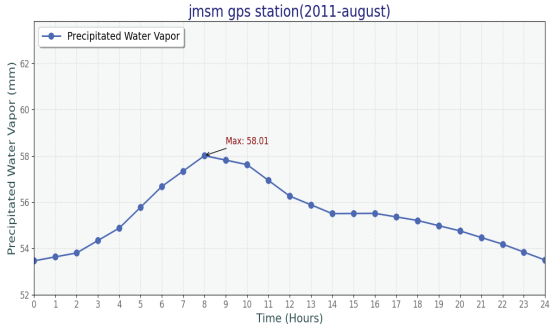

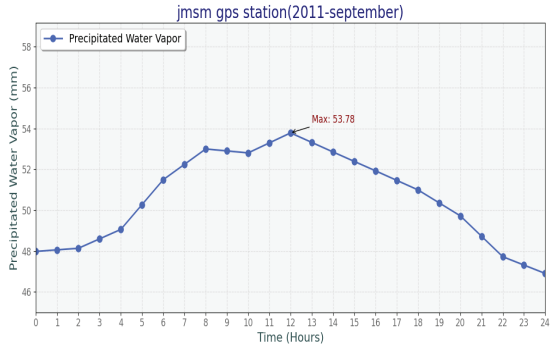

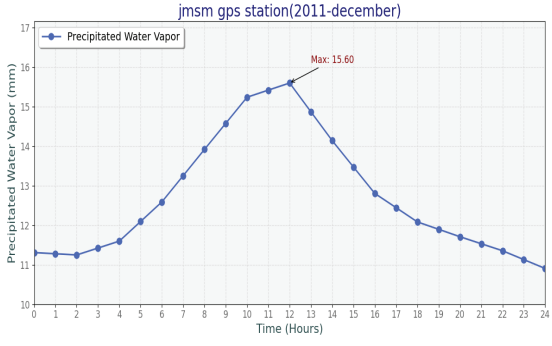

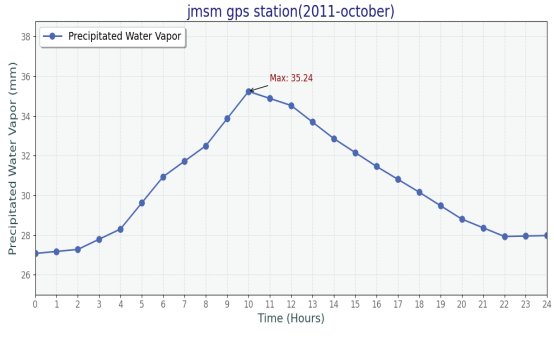

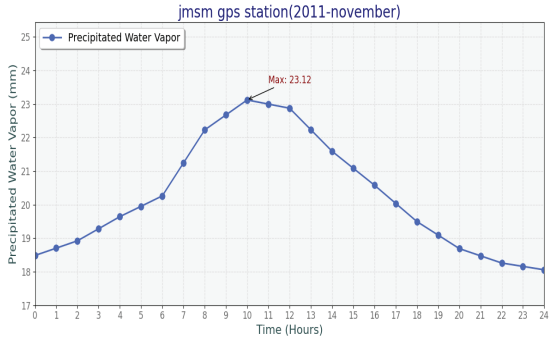

From the time series of the jmsm station, the maximum precipitated water vapour is 53.78 mm during the period of noon and the least maximum in January with precipitated water vapour of 5.75 mm during the period of 10-12 PM. A similar pattern is observed in the monthly analysis as the precipitated water vapour increases from January reaches a maximum in September and then starts decreasing till December.

The monthly maximum PWV of both stations is shown in the following table:

Table 2:

Month	GRHI	Time	JMSM	Time	Season
January	13.57	10 AM	5.75	10 AM	Winter
February	17.8	10 AM	8.92	10 AM	Winter
March	22.55	12 AM	14.80	12 PM	Winter-Spring
April	29.27	12 PM	16.77	12 PM	Spring
May	43.2	10 AM	22.19	12 PM	Spring-Summer
June	56.25	10 AM	25.56	12 PM	Summer
July	60.37	10 AM	27.05	10 AM	Summer-Monsoon
August	55.40	12PM	58.01	8 AM	Monsoon
September	39.76	12 PM	53.78	12 PM	Autumn
October	27.25	10 AM	35.24	10 AM	Autumn
November	18.19	12 PM	23.12	10 AM	Autumn
December	11.26	12 PM	15.6	12 PM	Winter

From Table 2 we can also observe that the maximum precipitated water vapour in the atmosphere is in the period between 10 AM to 12 PM throughout 2011 but in August the precipitated water vapour was maximum at 8 AM for JMSM station which may be due to the heavy rainfall in the month of July-September.

The graph illustrates that during the summer and monsoon seasons, the water vapour amount was at its highest; during winter, it recorded its lowest values. These increased pwv levels are due to orographic lifts in the mountain region; as air masses rise over hills and mountains, they cool down, causing condensation and precipitation (Serrano-Vincenti et al., 2022). The Terai is situated at the foothills of the Himalayas, adjacent to the Indo-Gangetic Plains. This location allows it to receive moisture-laden winds from the Bay of Bengal. During the monsoon season, the combination of warm temperatures and abundant moisture leads to high PWV levels, which can result in longer heavy rainfall. This moisture can lead to increased humidity, affect local weather patterns, and play a crucial role in the monsoon season in Nepal. An increase in altitude results in the condensation of water vapour in the atmosphere, which eventually precipitates as dew on the ground. In addition, while moving from south to north and gaining altitude, the dry air from the Tibetan plateau decreases the PWV, thus causing it to decrease (Ichiyanagi et al., 2007). Another reason can be drawn from the topography of Nepal. The Hilly and Himalayan area consists of high mountains and ranges. Most of the seasonal winds are intercepted by these slopes, which block the water vapour from effectively reaching the hilly and mountainous areas (Barros & Lang, 2003).

4. Conclusion

The Indian summer monsoon contributes to over 80% of Nepal's yearly precipitation. The intense rainfall in Nepal is primarily driven by humidity from the Arabian Sea (AS) and the Bay of Bengal (BoB) (Bohlinger et al., 2017; Boschi and Lucarini, 2019). As climate change progresses, the level of water vapour in the atmosphere is anticipated to rise, generating scientific curiosity about the effects of atmospheric water vapour on shifting moisture trends (Hoffmann et al., 2001). In this paper, The Terai lowland region showed a higher amount of precipitated water vapour from May to September, reaching its maximum in June and July. During that period, Nepal experiences monsoon rains. Conversely, the hilly region of Nepal gets noticeably less rainfall than the Terai from August to October, peaking in August and September.

From this research paper, we investigate the key things:

- Relatively less precipitated in the high altitude as compared to low altitudes
- Great significance for indication for the prediction of rainfall and severe weather
- Factor affecting the moisture content how is PWV pattern in the Himalayan region i.e. (topographic factor)
- The graph shows that there is a direct relationship between the PWV and monsoon rainfall.

Acknowledgement

The authors acknowledge their gratitude to the UNAVCO for their free access to raw data and thanks to the Massachusetts Institute of Technology (MIT) for providing the GAMIT tool. We would like to express our gratitude to my family and friends for their invaluable guidance and support and lastly to thank the Department of Physics, St. Xavier's College for providing their support.

References

Barros, A. P., & Lang, T. J. (2003). Monitoring the Monsoon in the Himalayas: Observations in Central Nepal, June 2001. https://journals.ametsoc.org/view/journals/mwre/131/7/1520-0493_2003_131_1408_mtmith_2.0.co_2.xml

Bevis, M., Businger, S., Chiswell, S., Herring, T. A., Anthes, R. A., Rocken, C., & Ware, R. H. (1994). GPS Meteorology: Mapping Zenith Wet Delays onto Precipitable Water. https://journals.ametsoc.org/view/journals/apme/33/3/1520-0450_1994_033_0379_gmmzwd_2_0_co_2.xml

Bevis, M., Businger, S., Herring, T. A., Rocken, C., Anthes, R. A., & Ware, R. H. (1992). GPS meteorology: Remote sensing of atmospheric water vapour using the global positioning system. *Journal of Geophysical Research: Atmospheres*, 97(D14), 15787–15801. https://doi.org/10.1029/92JD01517

Bohlinger, P., & Sorteberg, A. (2017). A comprehensive view on trends in extreme precipitation in Nepal and their spatial distribution: RAINFALL TRENDS IN NEPAL. *International Journal of Climatology*, 38. https://doi.org/10.1002/joc.5299

Boschi, R., & Lucarini, V. (2019). Water Pathways for the Hindu-Kush-Himalaya and an Analysis of Three Flood Events. Atmosphere, 10(9), 489. https://doi.org/10.3390/atmos10090489

Businger, S., Chiswell, S. R., Bevis, M., Duan, J., Anthes, R. A., Rocken, C., Ware, R. H., Exner, M., VanHove, T., & Solheim, F. S. (1996). The Promise of GPS in Atmospheric Monitoring. https://journals.ametsoc.org/view/journals/bams/77/1/1520-0477_1996_077_0005_tpogia_2_0_co_2.xml

Chapman, K. (2024, September 5). Terrain and Topography of Nepal: mountains, valleys, and plains. Earth Site Education. https://www.earth-site.co.uk/Education/terrain-and-topography-of-nepal-mountains-valleys-and-plains/

Chen, Y., Wen, J., Liu, R., Zhou, J., & Liu, W. (2022). The Characteristics of Water Vapor Transport and Its Linkage with Summer Precipitation over the Source Region of the Three Rivers. https://doi.org/10.1175/JHM-D-21-0095.1

Davis, J. L., Herring, T. A., Shapiro, I. I., Rogers, A. E. E., & Elgered, G. (1985). Geodesy by radio interferometry: Effects of atmospheric modelling errors on estimates of baseline length. *Radio Science,* 20(6), 1593–1607. https://doi.org/10.1029/RS020i006p01593

Ghimire, B. D., Gautam, B., Chapagain, N. P., & Bhatta, K. (2022). Annual and semi-annual variations of TEC over Nepal during the period of 2007–2017 and possible drivers. *Acta Geophysica*, *70*(2), 929-942.

Ghimire, B. D., & Chapagain, N. P. (2022). Ionospheric anomalies due to Nepal earthquake-2015 as observed from GPS-TEC data. *Geomagnetism and Aeronomy*, *62*(4), 460-473.

Ghimire, B. D., Wagle, S., & Thakur, P. (2024). Ionospheric and meteorological response to total solar eclipses. *Journal of Atmospheric and Solar-Terrestrial Physics*, *262*, 106292.

Hagemann, S., Bengtsson, L., & Gendt, G. (2003). On the determination of atmospheric water vapour from GPS measurements. Journal of Geophysical Research: Atmospheres, 108(D21). https://doi.org/10.1029/2002JD003235

Herring, T. A., King, R. W., Floyd, M. A., & McClusky, S. C. (2002). GAMIT: Reference Manual. *Massachusetts Institute of Technology.* http://www-gpsg.mit.edu/gg/docs/GAMIT_Ref.pdf

Hofmann-Wellenhof, B., Lichtenegger, H., & Collins, J. (2001). Global Positioning System. *Springer*. https://doi.org/10.1007/978-3-7091-6199-9

Ichiyanagi, K., Yamanaka, M. D., Muraji, Y., & Vaidya, B. K. (2007). Precipitation in Nepal between 1987 and 1996. *International Journal of Climatology*, 27(13), 1753–1762. https://doi.org/10.1002/joc.1492

Kursinski, R., A. Hajj, H., Leroy, S., & Herman, B. (2020). The GPS Radio Occultation Technique. Terrestrial, Atmospheric and Oceanic Sciences (TAO), 11. https://doi.org/10.3319/TAO.2000.11.1.53(COSMIC)

Manabe, S., & Wetherald, R. T. (1967). Thermal Equilibrium of the Atmosphere with a Given Distribution of Relative Humidity. https://journals.ametsoc.org/view/journals/atsc/24/3/1520-0469_1967_024_0241_teotaw_2_0_co_2.xml

Neelin, J. D., Martinez-Villalobos, C., Stechmann, S. N., Ahmed, F., Chen, G., Norris, J. M., Kuo, Y.-H., & Lenderink, G. (2022). Precipitation Extremes and Water Vapor. *Current Climate Change Reports*, 8(1), 17–33. https://doi.org/10.1007/s40641-021-00177-z

Niell, A. E. (1996). Global mapping functions for the atmosphere delay at radio wavelengths. *Journal of Geophysical Research*: Solid Earth, 101(B2), 3227–3246. https://doi.org/10.1029/95JB03048

Obregón, M. Á., Serrano, A., Costa, M. J., & Silva, A. M. (2021). Global Spatial and Temporal Variation of the Combined Effect of Aerosol and Water Vapour on Solar Radiation. *Remote Sensing,* 13(4), 708. https://doi.org/10.3390/rs13040708

Pokharel, N. (2023). A Study of Climate Change and Meteorological Analysis in Different Ecological Regions of Nepal. Bharatpur Pragya: *Journal of Multidisciplinary Studies*, 65–90. https://doi.org/10.3126/bpjms.v1i1.55499

Priester, W., Martin, H. A., & Kramp, K. (1960). Earth Satellite Observations and the Upper Atmosphere: Diurnal and Seasonal Density Variations in the Upper Atmosphere. Nature, 188(4746), 202–204. https://doi.org/10.1038/188202a0

Qiao, C., Liu, S., Huo, J., Mu, X., Wang, P., Jia, S., Fan, X., & Duan, M. (2023). Retrievals of precipitable water vapour and aerosol optical depth from direct sun measurements with EKO MS711 and MS712 spectroradiometers. Atmospheric Measurement Techniques, 16(6), 1539–1549. https://doi.org/10.5194/amt-16-1539-2023

Raval, A., & Ramanathan, V. (1989). Observational determination of the greenhouse effect. *Nature*, 342(6251), 758–761. https://doi.org/10.1038/342758a0

Rocken, C., Ware, R., Van Hove, T., Solheim, F., Alber, C., Johnson, J., Bevis, M., & Businger, S. (1993). Sensing atmospheric water vapour with the global positioning system. *Geophysical Research Letters,* 20(23), 2631–2634. https://doi.org/10.1029/93GL02935

Serrano-Vincenti, S., Condom, T., Campozano, L., Escobar, L. A., Walpersdorf, A., Carchipulla-Morales, D., & Villacís, M. (2022). Harmonic Analysis of the Relationship between GNSS Precipitable Water Vapor and Heavy Rainfall over the Northwest Equatorial Coast, Andes, and Amazon Regions. Atmosphere, 13(11), 1809. https://doi.org/10.3390/atmos13111809

Zumberge, J. F., Watkins, M. M., & Webb, F. H. (1997). Characteristics and Applications of Precise GPS Clock Solutions Every 30 Seconds. *NAVIGATION,* 44(4), 449–456. https://doi.org/10.1002/j.2161-4296.1997.tb02360.x